Michigan Technological University

Digital Commons @ Michigan Tech

Michigan Tech Publications

1-1-2017

Quantitating active photosystem II reaction center content from fluorescence induction transients

Cole D. Murphy
Mount Allison University

Guangyan Ni
Mount Allison University

Gang Li
Mount Allison University

Audrey Barnett
Michigan Technological University

Kui Xu
Mount Allison University

See next page for additional authors

Follow this and additional works at: https://digitalcommons.mtu.edu/michigantech-p

Part of the Geological Engineering Commons, and the Mining Engineering Commons

Recommended Citation

Murphy, C., Ni, G., Li, G., Barnett, A., Xu, K., Grant-Burt, J., Liefer, J., Suggett, D., & Campbell, D. (2017). Quantitating active photosystem II reaction center content from fluorescence induction transients. *Limnology and Oceanography: Methods, 15*(1), 54-69. http://doi.org/10.1002/lom3.10142
Retrieved from: https://digitalcommons.mtu.edu/michigantech-p/3761

Follow this and additional works at: https://digitalcommons.mtu.edu/michigantech-p

Part of the Geological Engineering Commons, and the Mining Engineering Commons

Authors

Cole D. Murphy, Guangyan Ni, Gang Li, Audrey Barnett, Kui Xu, Jessica Grant-Burt, Justin D. Liefer, David J. Suggett, and Douglas A. Campbell

This article is available at Digital Commons @ Michigan Tech: https://digitalcommons.mtu.edu/michigantech-p/3761

LIMNOLOGY
and
OCEANOGRAPHY: METHODS

ASLO

Limnol. Oceanogr.: Methods 15, 2017, 54–69
© 2016 The Authors Limnology and Oceanography: Methods published by Wiley Periodicals, Inc. on behalf of Association for the Sciences of Limnology and Oceanography
doi: 10.1002/lom3.10142

Quantitating active photosystem II reaction center content from fluorescence induction transients

Cole D. Murphy,[1] Guangyan Ni,[1,2] Gang Li,[1,3] Audrey Barnett,[4] Kui Xu,[1] Jessica Grant-Burt,[1] Justin D. Liefer,[1] David J. Suggett,[5] Douglas A. Campbell*[1]

[1]Biochemistry and Chemistry, Biology, and Environmental Science, Mount Allison University, Sackville, New Brunswick, Canada
[2]Key Laboratory of Vegetation Restoration and Management of Degraded Ecosystems, South China Botanical Garden, CAS, Guangzhou, China
[3]Key Laboratory of Tropical Marine Bio-resources and Ecology, South China Sea Institute of Oceanology, CAS, Guangzhou, China
[4]Michigan Technological University, Houghton, Michigan
[5]Climate Change Cluster (C3), University of Technology, Sydney, New South Wales, Australia

Abstract

Photosystem II (PSII) is a pigment-protein complex that photochemically extracts electrons from water, generating the reductant that supports biological productivity in all biomes. Estimating the content of active PSII reaction centers in a liquid sample is a key input for estimating aquatic photosynthesis rates, as well as for analyzing phytoplankton stress responses. Established procedures for PSII content quantification based on oxygen evolution are slow, imprecise and require dense cell suspensions, and are thus inapplicable to many laboratory or field studies. A new approach uses baseline chlorophyll fluorescence emission divided by the effective absorbance cross section for PSII photochemistry, with both variables derivable from single turnover fluorescence induction protocols. This approach has not been widely tested and is potentially subject to variation in samples suffering progressive photoinactivation or induction of non-photochemical quenching under variable light. We evaluated the validity of this approach for a marine picocyanobacteria, low and high light *Prochlorococcus* ecotypes, arctic and temperate prasinophyte green alga and two centric diatoms, generating 209 paired determinations from a range of growth and treatment conditions. We successfully calibrated the fluorescence derived estimator for PSII reaction center content, and demonstrate a modification that corrects for the short term influence of photoinactivation. The modified parameter shows little response to induction of non-photochemical quenching. In doing so we show the potential and limitations of an estimator of active PSII reaction center content that is sufficiently robust to support rapid, time-resolved autonomous measures of primary productivity from lakes and oceans.

Photosystem II (PSII), acting in tandem with PSI, photochemically generates the reductant that fuels productivity to drive biogeochemical nutrient cycling throughout aquatic biomes (Falkowski et al. 2008). Rapid and scalable estimates of the rate of photochemical reductant generation *per* active PSII reaction center are now well established on the basis of quasi-instantaneous measurements from chlorophyll *a* fluorescence induction and incident light (Suggett et al. 2009a; Huot and Babin 2010; Lawrenz et al. 2013). However, a more biogeochemically meaningful determinant is the rate of photochemical electron generation by PSII per volume (or per chlorophyll). For this, fluorescence induction measurements of electron generation rate per PSII must be scaled by content of active PSII ($[PSII]_{active}$) per volume (or per chlorophyll), a factor that is highly variable across both algal taxa and growth conditions (Suggett et al. 2010).

While immunoblotting techniques can determine absolute abundance of the protein subnits of PSII (Brown et al. 2008; Macey et al. 2014), they do not account for the variable fraction of total PSII protein that is part of a photochemically active PSII reaction center contributing to sustained electron transport (Smith et al. 1990; Wu et al. 2011, 2012; Campbell et al. 2013). Consequently, the most popular method to yield an absolute measure of $[PSII]_{active}$ is from oxygen flash yield based approaches (Chow et al. 1989; Suggett et al. 2009a) (Fig. 1). These approaches are time intensive, requiring at least 15 min to perform per sample, but also require that samples be concentrated into dense cell suspensions to measure sufficient changes

*Correspondence: dcampbell@mta.ca

This is an open access article under the terms of the Creative Commons Attribution-NonCommercial License, which permits use, distribution and reproduction in any medium, provided the original work is properly cited and is not used for commercial purposes.

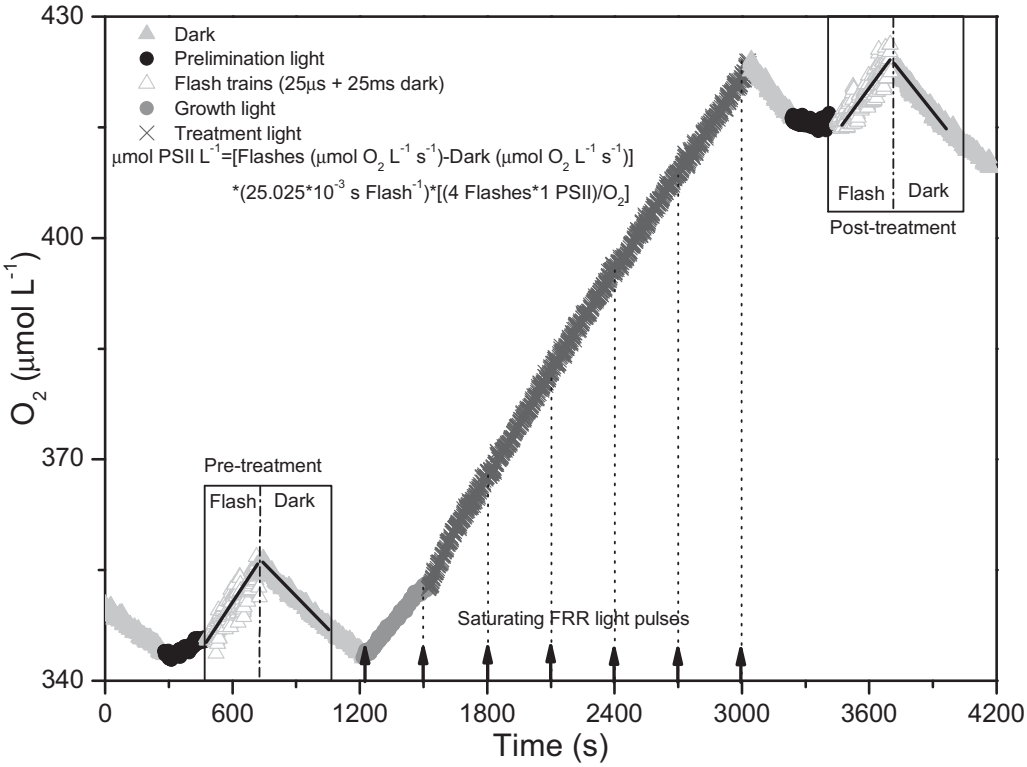

Fig. 1. Representative O_2 flash yield data and treatment time course. Oxygen concentration plotted vs. time over a light treatment timecourse. Phytoplankton cell suspension was loaded into a 1 cm cuvette with a micro stir bar in the bottom. A tightly fitted temperature control plug was mounted with a solid state optode O_2 sensor projecting into the sample volume. The cuvette assembly was then placed into an LED optical unit equipped with a magnetic stirring unit. Cell suspension was initially exposed to 300 s darkness for measurement of dark respiration, followed by a period of low light pre-illumination to activate photosynthesis, and then a flash train (9600 single turnover saturating flashes, each flash lasts 25 μs, interspersed by 25 ms dark) to provoke saturating single turnovers of PSII photochemistry (Chow et al. 1989; Suggett et al. 2009a; Oxborough et al. 2012). In trial runs, we varied the light level and duration of the flashes to ensure they were saturating (data not shown). After the flash train, cells were again exposed to darkness and respiration immediately measured to approximate the rate of respiration prevailing during the flash train. The difference in O_2 slope between the flash train and subsequent darkness was then used to estimate active $[PSII]_{active}$ content in the sample under culture growth conditions. We then exposed cells to consecutive periods of 300 s under a treatment light level. At the end of each 300 s period an FRR induction (Fig. 2) was applied. In parallel, we continued to use the optode to track O_2 evolution under the treatment light levels. After the light treatment, cells were again pre-illuminated, and the O_2 flash yield protocol was repeated to estimate $[PSII]_{active}$ content after the light treatment. In this example figure, cells were arctic *Micromonas* NCMA 2099 growing at 10°C, 36 μmol photons m^{-2} s^{-1}, treated at 294 μmol photons m^{-2} s^{-1}, without lincomycin.

in oxygen evolution over time (Suggett et al. 2009a). Furthermore repeat measurements on the same culture are often variable in part because of short term variations in the underlying rates for consumption of oxygen through multiple paths (Campbell et al. 1999; Waring et al. 2010; Halsey et al. 2011; Roberty et al. 2014). In principle true oxygen evolution and consumption can be resolved simultaneously using water labelled with ^{18}O but the requisite membrane inlet mass spectrometer system is as yet complex to maintain and not suited to high throughput or under-way measures. Together such limitations generally preclude use of oxygen flash yields for tracking kinetic responses of cultures, let alone natural populations subjected to continually changing environmental conditions (Moore et al. 2006; Suggett et al. 2006).

Lack of robust and rapid determinations of $[PSII]_{active}$ is a major bottleneck toward widespread implementation of active fluorometry for aquatic productivity assessment. Efforts to empirically determine $[PSII]_{active}$ from fluorescence induction-based parameters have, until recently, been generally unsuccessful (Babin et al. 1996; Suggett et al. 2004, 2006). However, (Oxborough et al. 2012; Silsbe et al. 2015) recently demonstrated that since (a) F_0' (baseline fluorescence in the light adapted state; Fig. 2) is proportional to the total amount of pigment for all $PSII_{active}$ in a measured volume and (b) σ'_{PSII} (the effective absorbance cross section for PSII in the light adapted state; Fig. 2) is proportional to the amount of pigment associated with each PSII, the ratio F_0'/σ'_{PSII} is proportional to $[PSII]_{active}$ per volume. As such, $[PSII]_{active}$ can be inherently estimated from the fluorescence induction parameters themselves. While this demonstration potentially provides a major breakthrough in how active fluorescence induction techniques can be broadly applied to productivity studies, it has not been rigorously tested beyond these initial studies. We therefore tested the

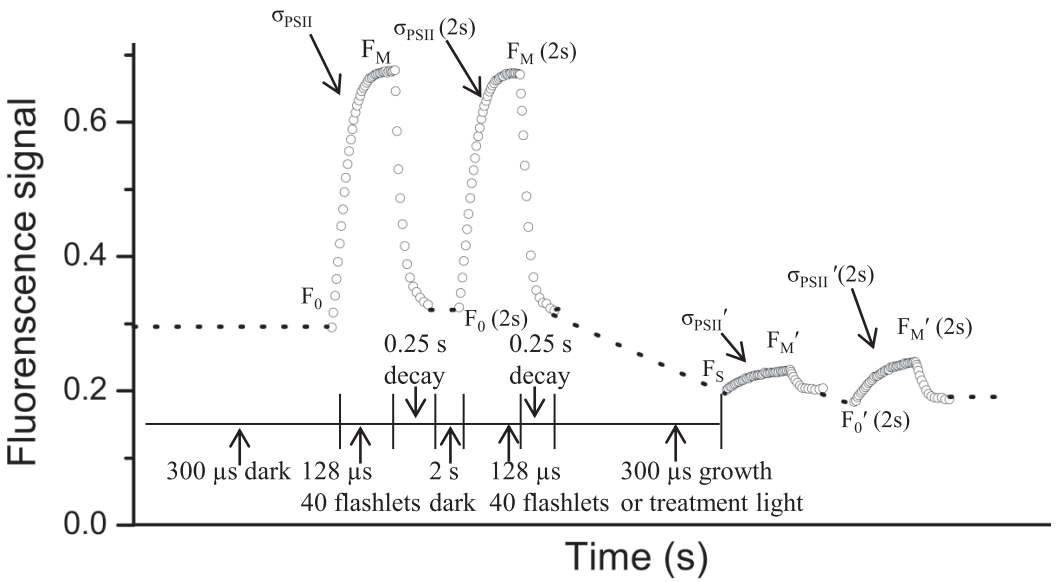

Fig. 2. Representative Chlorophyll Fluorescence fast repetition rate (FRR) induction traces. Arctic *Micromonas* NCMA 2099 grown at 2°C and 30 μmol photons m^{-2} s^{-1}. The initial dashed line tracks a 300 s dark acclimation followed by FRR induction provoked by a train of 40 flashlets (1.2 μs duration, 2 μs intervening dark) applied over 128 μs that cumulatively close Photosystem II (PSII). We use a curve fit (PSIWORX-R; http://sourceforge.net/projects/psiworx/) of this initial FRR induction trace to extract the parameters F_0, the basal fluorescence in the dark acclimated state, F_M, the maximal fluorescence with all PSII closed, and the induction parameters σ_{PSII}, the effective absorbance cross section serving PSII photochemistry and ρ a parameter for excitation connectivity among PSII centers, in the dark acclimated state (Kolber et al. 1998; Laney 2003; Laney and Letelier 2008). Following the train of saturating flashlets our protocol slows the flash rate, allowing PSII to re-open over a 0.25 s span. After a further 2 s dark period to allow re-opening of PSII we applied a second FRR induction. The dashed line then spans a subsequent 300 s incubation under a treatment light (97 μmol photons m^{-2} s^{-1} in this example) ending with an FRR induction (open symbols) under exposure to the treatment light to define F_S, the fluorescence in the light acclimated state, F'_M, σ'_{PSII}, and ρ'. We then again applied an FRR induction after a further 2 s dark period to allow re-opening of closed PSII centers, for measurement of F'_{02s}, F'_{M2s}, and σ'_{PSII2s} Note that in these cells even 2 s of darkness allows some increase from F'_M to F'_{M2s}, reflecting partial relaxation of non-photochemical quenching within 2 s.

correlation between F'_0/σ'_{PSII} and $[PSII]_{active}$ in samples of opportunity across a diverse range of phytoplankton taxa which were grown under a range of conditions. We found an artefactual degradation of the correlation between F'_0/σ'_{PSII} and $[PSII]_{active}$ under conditions that induce net photoinactivation of PSII. We therefore developed a modified estimator, $[PSII]_{active}$ Fluor with improved performance across both uninhibited and inhibited samples. We furthermore show that $[PSII]_{active}$ Fluor shows only limited sensitivity to the induction of moderate levels of Non-Photochemical Quenching across a range of taxa. $[PSII]_{active}$ Fluor therefore supports rapid estimation of the content of active PSII across a wide range of taxa, growth histories and short-term changes in illumination.

Materials and methods

We examined a suite of phytoplankton taxa and growth conditions. Three picocyanobacteria strains, *Synechococcus* sp. WH8102, *Prochlorococcus marinus* MED4, and *P. marinus* MIT9313, obtained from the NCMA (Boothbay Harbour Maine) were grown as semi-continuous cultures under 30 or 260 μmol photons m^{-2} s^{-1} with a 12 : 12 L : D cycle, except for *P. marinus* MIT9313 grown only at 30 μmol photons m^{-2} s^{-1} since 260 μmol photons m^{-2} s^{-1} appeared to exceed its tolerable light range. Cultures were grown in a temperature controlled incubator (Percival Scientific) at 22°C (Table 1). *Synechococcus* sp. WH8102 was grown in PCR—S11 medium, prepared according to a modified recipe from the Roscoff Culture Collection in which the levels of Fe_3Cl were changed to 2 μmol L^{-1}. The two *Prochlorococcus* strains were grown in Pro99 medium prepared using the Pro99 kit from NCMA. All semi-continuous cultures were maintained as 75 mL, inoculated with 15 mL from the previous culture and 65 mL of the appropriate medium, and later used to establish larger working cultures (250 mL total volume), with a one in five dilution of parent culture in appropriate medium.

Two strains of the prasinophyte *Micromonas*, were grown with 12 : 12 L : D cycles, in 6-well plates containing 6.5 mL of batch culture per well in incubators. The temperate origin NCMA 1646 was grown at 20°C under 36 and 185 μmol photons m^{-2} s^{-1} light intensity whereas the arctic origin NCMA 2099 was grown at 2 and 10°C under 36 μmol photons m^{-2} s^{-1} intensity. These strains were obtained from the Provasoli-Guillard National Center of Marine Phytoplankton and cultured in L1-Si medium prepared using filtrated seawater according to (Keller et al. 1987; Guillard and Hargraves 1993). The prasinophyte *Ostreococcus tauri* (RCC745) was

Table 1. Summary of phytoplankton strains, growth, and treatment conditions.

Strain	Growth temperature (°C)	Growth light (μmol photons m^{-2} s^{-1})	Treatment light (μmol photons m^{-2} s^{-1})	Nitrate
Synechococcus sp. WH8102	22	25, 30, 75, 150, 260, 300	260	Replete
Prochlorococcus sp. MIT9313	22	30, 90	260	Replete
Prochlorococcus sp. MED4	22	30, 260	260	Replete
Micromonas NCMA1646	20	36, 185	74, 100, 140, 192, 388, 470, 550, 734	Replete
Micromonas NCMA2099	2, 10	36	74, 87, 153, 192, 286	Replete
Ostreococcus tauri RCC745	18	100	260	Replete; early stationary
Thalassiosira pseudonana CCMP1335	18	30, 180, 380	NA	Excess; replete
Thalassiosira punctigera CCAP1085/19	18	25, 30, 75 90, 150, 180, 300	NA	Replete; limited

obtained from the Roscoff Culture Collection and cultured in f/2 medium (Guillard and Ryther 1962) using filtered seawater and modified to contain 120 μmol L^{-1} NO_3^-; 50% less PO_4^{3-}, trace metals, and vitamins; 1 mmol L^{-1} $NaHCO_3$; and no added Si and was sterilized by filtration through a 0.2 μm capsule filter under sterile conditions. *O. tauri* was grown with a 12 : 12 L : D cycle, under 100 μmol photons m^{-2} s^{-1} light intensity at 18°C in 5 L glass bioreactors that received gentle stirring from PTFE stir bars (~ 60 RPM) and bubbled with air. *O. tauri* cultures were sampled during nutrient replete exponential growth and at the nitrogen limited stationary phase.

Two marine centric diatom strains *Thalassiosira pseudonana* (CCMP 1335) and *Thalassiosira punctigera* (CCAP 1085/19) were obtained from the Provasoli-Guillard National Center of Marine Phytoplankton and cultured in rectangular cuvettes (450 mL volume) of FMT-150 photobioreactors with 2 cm optical pathlength for illumination from a flat array of blue LED lights facing the rear of the cuvette (Photon Systems Instruments, Drasov, Czech Republic) at 18°C. These strains were grown in two different media: enriched artificial seawater (~ 550 μmol L^{-1} NO_3^-) (Berges et al. 2001), originally from (Harrison et al. 1980), except with 54.5 μmol L^{-1} Si and 0.82 μmol L^{-1} Sr to limit precipitation during autoclaving; or the same ESAW except with one tenth of the nitrogen content (~55 μmol L^{-1} NO_3^-), corrected with sodium bicarbonate to yield an equivalent total alkalinity. We gently mixed the cultures with a curtain of bubbles emitted from four apertures across the cuvette bottom with outdoor fresh air that was filtered through a 0.2 μm micro-filter and bubbled through sterile distilled water for humidification before entering the culture cuvette. We provided continuous growth light measured with a microspherical quantum sensor (US-SQS, Walz, Germany). Light intensities within the culture vessels filled with media were set to 30, 180, and 380 μmol photons m^{-2} s^{-1} for *T. pseudonana*, or to 30, 90, and 180 μmol photons m^{-2} s^{-1} for *T. punctigera*.

We initially sparged a 3 mL cell suspension taken from the culture vessel with gaseous nitrogen to lower the dissolved oxygen content of the sample. The sparged cell suspension was placed, along with a micro stir bar, into a 4 mL cuvette with 1 cm path length and four clear sides, which was then sealed with a custom fabricated aluminum plug. The plug was used to control the sample volume at the appropriate growth temperature (2, 10, 18, 20, or 22°C depending on the culture) through plumbed connections to a circulating thermostatted bath. The cuvette assembly was mounted within a Super Head unit of a PSI FL3500 fluorometer (Photon Systems Instruments, Czech Republic) whose LED sources were used to apply pre-illumination, actinic light, single turnover saturating flashes, and trains of flashlets for fast repletion and relaxation (FRR) fluorescence inductions.

Dissolved oxygen concentration in the sealed cuvette assembly was tracked using a FireSting Optode sensor controlled through Oxygen Logger software (PyroScience) during measurement and treatment protocols, with a representative progression outlined in Fig. 1. We tracked oxygen consumption in the dark and then applied a low pre-illumination (20 μmol photons m^{-2} s^{-1}) to induce photosynthetic electron transport. We then stopped the pre-illumination and immediately applied a train of 9400 saturating single turnover flashes of 25 μs duration, spaced every 25,000 μs, after which dark respiration was also measured, allowing us to estimate the content of active PSII mL^{-1} in the sample following the oxygen flash yield approach (Chow et al. 1989; Suggett et al. 2009a). We performed pilot experiments for each taxon to determine the saturating single turnover flash intensity, flash duration and flash repeat timing for saturation of the response of oxygen evolution per flash (data not shown) such that for every four flashes 1 O_2 is produced per photochemically active PSII in the sample suspension. From the net oxygen evolution during the flash train and the immediately subsequent dark respiration we estimated the gross

oxygen evolution during the flash train period. This approach enabled us to calculate PSII reaction center content per unit volume as:

$$\mu\text{mol PSII L}^{-1} = \mu\text{mol O}_2\text{s}^{-1}\text{L}^{-1} \times (25.025 \times 10^{-3}\text{s Flash}^{-1}) \times (4 \text{ Flash } 1 \times 1 \text{ PSII/O}_2)$$

Immediately following the oxygen flash yield determination of μmol PSII L^{-1} we applied FRR fluorescence inductions to the cell suspension and recorded the data using the FluorWin software (Photon Systems Instruments, Czech Republic) (Fig. 2). Each FRR induction was comprised of an initial series of 40 FRR flashlets of 1.2 μs duration each separated by 2 μs (representative traces in Fig. 2). Each flashlet was ca. 65,000 μmol photons m^{-2} s^{-1} intensity, with flashlet intensity optimised for each culture type so that a train of 40 FRR flashlets over 128 μs delivered sufficient cumulative excitation power to drive PSII fluorescence to saturation (maximum yield) within ca. 30 flashlets and thus ensure robust retrieval of parameters (Laney 2003) from the physiological model fit to each FRR induction. The initial FRR induction was followed by a 2 s dark interval to fully re-open all PSII reaction centers, followed by a second FRR induction with open PSII reaction centers but the sample only partially relaxed from the light-adapted state. FRR inductions were performed for samples in the dark and then again for samples under periods of actinic light (Fig. 2).

All FRR fluorescence induction curves were imported from the Photon Systems Instrument FluorWin data output and fit to the four parameter model of (Kolber et al. 1998) using the PSIWORX-R package implemented in the *R* scripting language (www.sourceforge.net) For each set of FRR inductions (Fig. 2) we determined the maximum fluorescence (F_M in the dark, F'_M at the applied light, F'_M2s after 2 s of dark), the baseline fluorescence (F_0 in the dark, F_S at the applied light light, $F'_0$2s after 2 s of dark), the effective absorbance cross section for PSII (σ_{PSII} in the dark, σ'_{PSII} at the applied light, and σ'_{PSII}2s after 2 s of dark) and the connectivity of the antenna for PSII (ρ in the light, ρ' at the applied light, and ρ'2s after 2 s of dark). We calibrated the intensity of the FRR flashlets for each fluorometer unit and supplied the calibration data to PSIWORX-R for estimation of absolute σ_{PSII} values with units of A^2 $PSII^{-1}$.

For comparability across samples from different taxa and different growth conditions we settled on F'_0 2s as our parameter to approximate F'_0, the level of fluorescence in light-acclimated cells, with PSII open. F'_0 has long been problematic to estimate (Campbell et al. 1998) because it requires judgement to decide how long a dark interval to apply to allow PSII to re-open while retaining the samples in their light acclimated state, in the face of rapid changes in non-photochemical quenching (Lavaud 2007), state transitions (Campbell et al. 1998), and other rapid shifts in photophysiology. A dedicated instrument control script might be applied to improve the F'_0 estimate but in our dataset across multiple taxa and growth conditions F'_0 2s proved our most robust general estimator for F'_0, particularly since we included data from arctic phytoplankton with massive induction of Non-Photochemical Quenching and relatively slow re-opening of PSII after actinic illumination (Table 1). Since we chose F'_0 2s to provide our estimator for F'_0, we used the parallel measures for effective absorption (σ'_{PSII} 2s) to thus yield our ratio F'_0 2s/σ'_{PSII} 2s, since F'_0 2s and σ'_{PSII} 2s are derived from exactly the same FRR induction curve (Fig. 2) for best internal consistency in measurements. To compare measures performed on different samples on three different fluorometer units the F'_0 2s values were calibrated to equivalent excitation flashlet levels (Silsbe et al. 2015).

Using these parameters a relative measure of $[PSII]_{active}$ content, F'_0 2s/σ'_{PSII} 2s was calculated for each sample under steady state growth conditions, based on the assumptions that F_0 is proportional to the total pigment for all PSII centers, and that σ_{PSII} is proportional to the pigment associated with each PSII (Oxborough et al. 2012; Silsbe et al. 2015). Thus, the ratio of F'_0 2s/σ'_{PSII} 2s is proportional to the total number of PSII.

Most cell suspensions were then maintained in the sealed cuvette and subjected to a higher light treatment (Fig. 1) without or with 500 μg mL^{-1} lincomycin to block PSII repair (Tyystjärvi et al. 2002; Hakkila et al. 2014). This additional step enabled us to analyze the effects of PSII photoinactivation in the absence of repair (presence of lincomycin) and responses to high light in the presence of repair (in the absence of lincomycin). FRR fluorescence measures were repeated every 327 s during the high light treatment. At the end of the high light treatment another oxygen flash yield protocol was run to determine the final content of $[PSII]_{active}$.

Chlorophyll *a* content was determined from each sample suspension just prior to any measurement, and subsequently from all of the post treatment sample suspensions. For all strains except *O. tauri* RCC 745, 100 μL of cell suspension was placed in 90% acetone saturated with $MgCO_3$ for extraction, immediately wrapped with aluminium foil and stored at −20°C until a spectrophotometric assay was performed (Jeffrey and Humphrey 1975; Ritchie 2006). For *O. tauri* RCC 745, 100 μL of cell suspension was frozen immediately in liquid nitrogen and chlorophyll *a* was extracted in 3 : 2 90% acetone : DMSO according to (Shoaf and Lium 1976) and quantified with a fluorometer (Turner AU-10) (Welschmeyer 1994).

Results and discussion

The ratio F'_0 2s/σ'_{PSII} 2s can be obtained with an FRR induction curve measured within 128 μs (Fig. 2), thereby permitting time resolved measurements of $[PSII]_{active}$ through dynamic physical environments including non-steady state

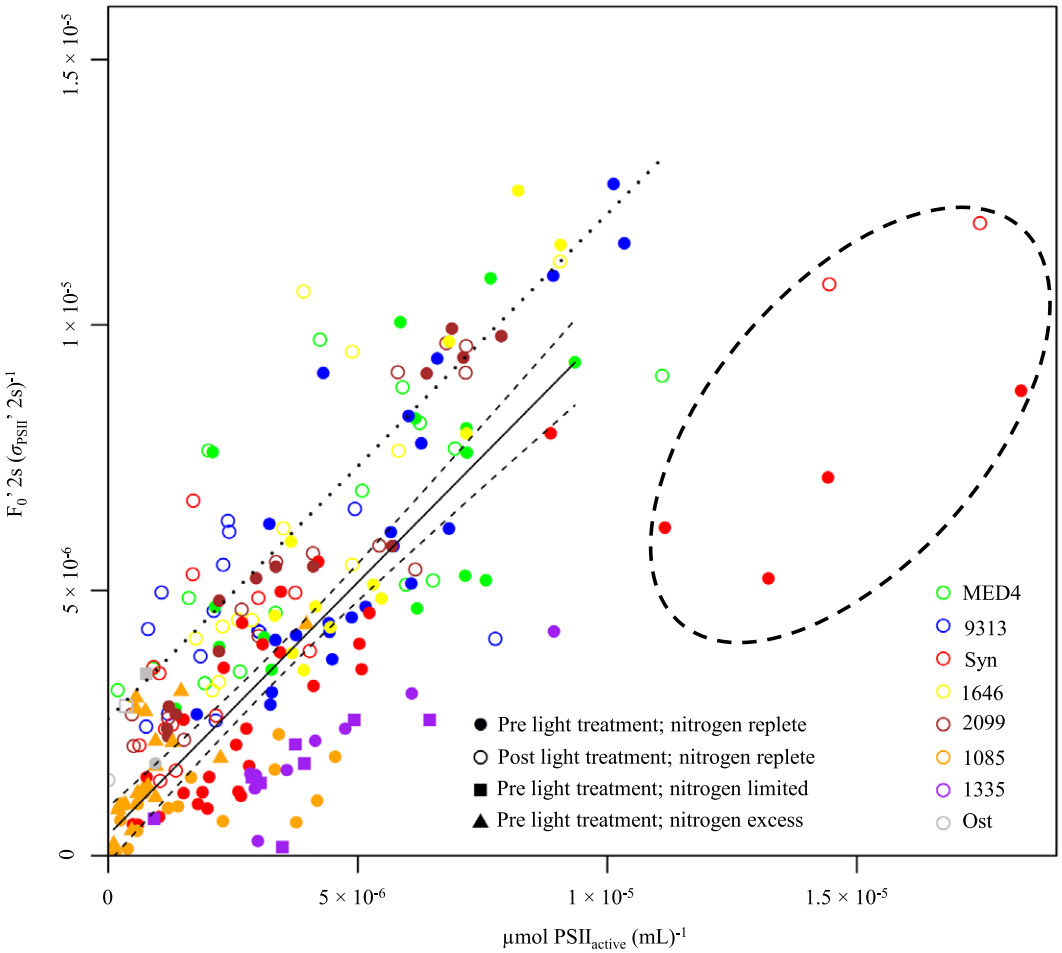

Fig. 3. The calibration of (F_0' 2s)/(σ'_{PSII} 2s) against the measured $[PSII]_{active}$ determined via oxygen flash yield measurements on the same samples. Filled symbols show measurements taken before the light treatment while the empty symbols show measurements taken after the light treatment, with or without lincomycin. Circles, squares, and triangles show samples grown under nitrogen replete, limited nitrogen, and excess nitrogen, respectively. The data is taken from eight taxa indicated by different colored points, *Prochlorococcus marinus* MED4; *Prochlorococcus marinus* MIT9313; *Synechococcus* sp. WH8102; *Micromonas* sp. NCMA1646; *Micromonas* sp. NCMA2099; *Ostreococcus tauri* RCC745; *Thalassiosira punctigera* CCAP1085/19; and *Thalassiosira pseudonana* CCMP 1335. The solid black line shows the regression through measurements taken under growth conditions, with dashed lines showing 95% confidence intervals, with a slope of 0.7120 ± 0.05249 and an intercept of $1.461 \times 10^{-6} \pm 2.588 \times 10^{-7}$and an R^2 of 0.5627. A statistically significant ($p < 0.05$) effect of the higher light treatment was seen on the intercept of the regression (dotted line) when fit to a linear model of (F_0' 2s)/(σ'_{PSII} 2s) against the measured $[PSII]_{active}$, with light treatment as a binary interaction term in the *R* scripting environment. Five measures taken from high-density cell suspensions of *Synechococcus* fell significantly below the regression (dotted oval) and were excluded from the regression.

treatments in the laboratory or under natural field sampling conditions. Such a fluorescence-based approach removes the requirement for concentrating samples into cell suspensions and can capture $[PSII]_{active}$ for any given cell suspension or population where F_0' and σ'_{PSII} can be robustly resolved. For comparisons across samples, or for quantitative estimates, F_0' 2s/σ'_{PSII} 2s must be calibrated against known $[PSII]_{active}$ (Oxborough et al. 2012; Silsbe et al. 2015). The measures of F_0' must be taken under defined fluorescence excitation intensities, excitation wavelength band and emission detection wavelength band (Simis et al. 2012), to avoid artefactual changes in measured F_0' independent of any change to the sample.

For our study we used a single fluorometer model (Photon Systems Instruments FL3500) running in FRR mode to deliver the excitation through 455 nm blue light LED with detection of chlorophyll fluorescence > 700 nm, thereby maintaining consistent excitation and emission wavelength bands across samples. However, to accommodate different sample suspension densities and effective absorbance cross sections we periodically had to vary the FRR excitation flashlet intensity among measurements. We therefore devised a calibration procedure by measuring F_0' at a range of different excitation flashlet intensities to then convert all F_0' measures from all samples back to a single equivalent flashlet excitation intensity. More sophisticated protocols for comparing

Table 2. Parameters and equations.

Parameter	Equation	Definition, units	Reference
F_0		Minimal fluorescence with PSII open	(van Kooten and Snel 1990)
F_M		Maximal fluorescence with PSII closed	(van Kooten and Snel 1990)
F_S		Fluorescence at an excitation level	(van Kooten and Snel 1990)
F'_M		Maximal fluorescence with PSII closed in at an excitation level	(van Kooten and Snel 1990)
F'_{M2s}		Maximal fluorescence with PSII closed 2 s after excitation	Figure 2
F'_{02s}		Minimal fluorescence with PSII open 2 s after excitation	Figure 2
F'_{0Oxbo}	$1/\{(1/F_0\ 2s - 1/F_M\ 2s + 1/F_M'\ 2s);$ $F_0\ 2s/\{(F_M\ 2s - F_0\ 2s)/(F_M\ 2s) + (F_0\ 2s)/(F_M'\ 2s)\}$	Minimal fluorescence with PSII open, estimated for cells under excitation, excluding cumulative influence of photoinactivation. F_0 2s & F_M 2s measured after exposure to low light level to avoid distortions from dark down regulation of PSII fluorescence	(Oxborough and Baker 1997; Ware et al. 2015a,b)
ρ		excitation connectivity among PSII centers	(Kolber et al. 1998)
σ_{PSII}		functional absorbance cross section for PSII photochemistry	(Kolber et al. 1998)
σ'_{PSII}		functional absorbance cross section for PSII photochemistry under excitation	(Kolber et al. 1998)
σ'_{PSII2s}		functional absorbance cross section for PSII photochemistry 2 s after excitation	Figure 2
σ_i	$[PSII]_{active}t = [PSII]_{active}t_0 * e^{(-\sigma i * t * I)}$	target size for photoinactivation of PSII across multiple excitation levels I, m^2 $photon^{-1}$	(Oliver et al. 2003; Key et al. 2010; Campbell and Tyystjärvi 2012)

measures across different taxa and different instruments can be found in Silsbe et al. (2015).

Calibration of F'_0/σ'_{PSII} using oxygen flash yield determination of $[PSII]_{active}$

For culture samples taken directly from their growth conditions (pre-light treatment) we observed a linear correlation (solid line; $R^2 = 0.5627$; slope $= 0.7120 \pm 0.05249$, y intercept $= 1.461 \times 10^{-6} \pm 2.588 \times 10^{-7}$; dotted lines show 95% confidence interval on regression) between F'_0 2s/σ_{PSII}' 2s vs. oxygen flash yield measures of $[PSII]_{active}$ mL^{-1} (Fig. 3) for seven diverse phytoplankters (Table 2). The regression was not significantly affected by measures taken from low nor higher growth light culture conditions ($p > 0.05$), nor by our range of taxa. These estimates on a volume basis include the influence of different cell suspension densities, and indeed we verified the linearity of the response using samples taken from the same cultures of *Synechococcus* WH8102 and *Prochlorococcus* MED4 but concentrated to a range of cell suspension densities, and through variations in sample cell suspension densities across our experiments. Five measures taken from high density, optically thick cell suspensions of *Synechococcus* fell significantly below the regression (dotted oval, Fig. 3). These samples did not reach saturation in the FRR induction curve because of excessive optical thickness relative to the flashlet intensity and so were excluded from the regression (points within dotted oval).

To remove the influence of cell suspension density we normalized both the F'_0 2s/σ'_{PSII} 2s and the oxygen flash yield measures of $[PSII]_{active}$ to the corresponding chlorophyll *a* content in each sample. While these data are plotted as their natural logarithm for graphical clarity (Fig. 4), we again

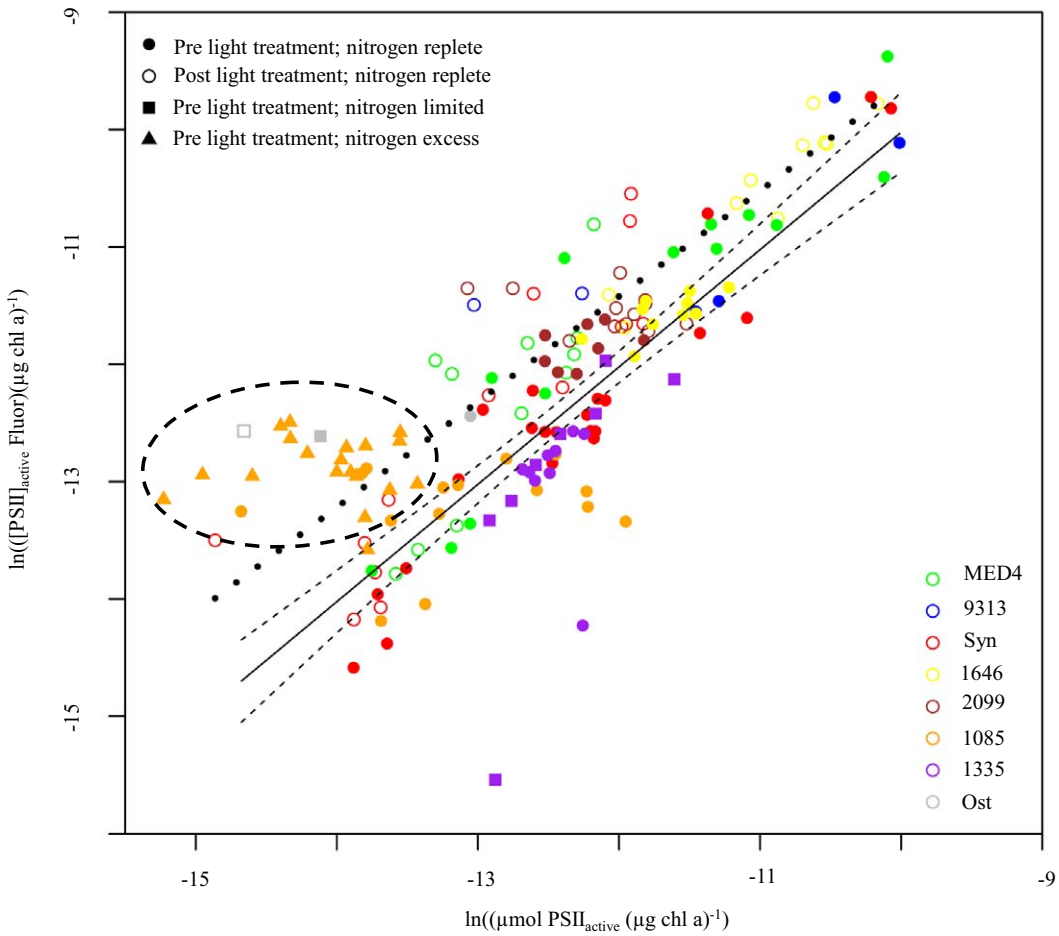

Fig. 4. The calibration of (F_0' 2s)/(σ'_{PSII} 2s) normalized to chlorophyll against the measured $[PSII]_{active}$ content determined via oxygen flash yield measurements normalized to chlorophyll. The data was transformed to natural logarithms to better visualize the trend. Filled symbols show measurements taken before a light treatment while the empty symbols show measurements taken after a light treatment, with or without lincomycin. Circles, squares, and triangles show samples grown under nitrogen replete, limited nitrogen, and excess nitrogen, respectively. The data is taken from eight taxa indicated by different coloured points, *Prochlorococcus marinus* MED4; *Prochlorococcus marinus* MIT9313; *Synechococcus* sp. WH8102; *Micromonas* sp. NCMA1646; *Micromonas* sp. NCMA2099; *Ostreococcus tauri* RCC745; *Thalassiosira punctigera* CCAP1085/19; and *Thalassiosira pseudonana* CCMP 1335. The solid black line shows the regression through the measurements taken at growth conditions, with dashed lines showing 95% confidence intervals. The non-transformed data show a linear correlation with a slope of 1.371 ± 0.06876 and an intercept $-1.310 \times 10^{-6} \pm 8.276 \times 10^{-7}$ was not significantly different from 0 ($p > 0.05$)and an R^2 of 0.8188. A statistically significant ($p < 0.05$) effect of the light treatment was seen on the intercept of the regression (dotted line) when fit to a linear model of (F_0' 2s)/(σ'_{PSII} 2s) against the measured $[PSII]_{active}$, with light treatment as a binary interaction term in the *R* scripting environment. Measures taken from excess-nitrogen cultures of *Thalassiosira punctigera* CCAP1085/19 and N-limited *Ostreococcus* were excluded from the regression of chlorophyll-normalized data.

found a strong correlation (solid line; $R^2 = 0.8188$, slope = 1.371 ± 0.06876; y intercept = $-1.310 \times 10^{-6} \pm 8.276 \times 10^{-7}$ and not significantly different from 0, $p > 0.05$; dotted lines show 95% confidence interval on regression) for non-log transformed data, for samples taken direct from growth conditions.

Together our analysis of a wide range of phytoplankton taxa and approach (F_0' 2s/σ_{PSII}' 2s) not only independently verifies, but also builds on, the previous demonstrations of retrieving PSII reaction center content through FRR fluorescence induction parameters (Oxborough et al. 2012, Silsbe et al. 2015). Our dataset for diatom cultures grown under nitrogen repletion or limitation remained on the regression but data from the diatom *T. punctigera* CCAP 1085/19 grown under excess nitrogen stress fell off the trend for the chlorophyll normalized regression, possibly due to dilute cell conditions resulting in poor chlorophyll *a* concentration determinations, and as such were excluded from regressions (points within dotted oval). The chlorophyll-normalized measures for nitrogen-limited *O. tauri* also fell somewhat above the regression (Fig. 4), albeit with limited replication. Further work is therefore needed to determine whether excess nitrogen stress (Drath et al. 2008) or nitrogen limitation stress (Moore et al. 2013) systematically disrupts the

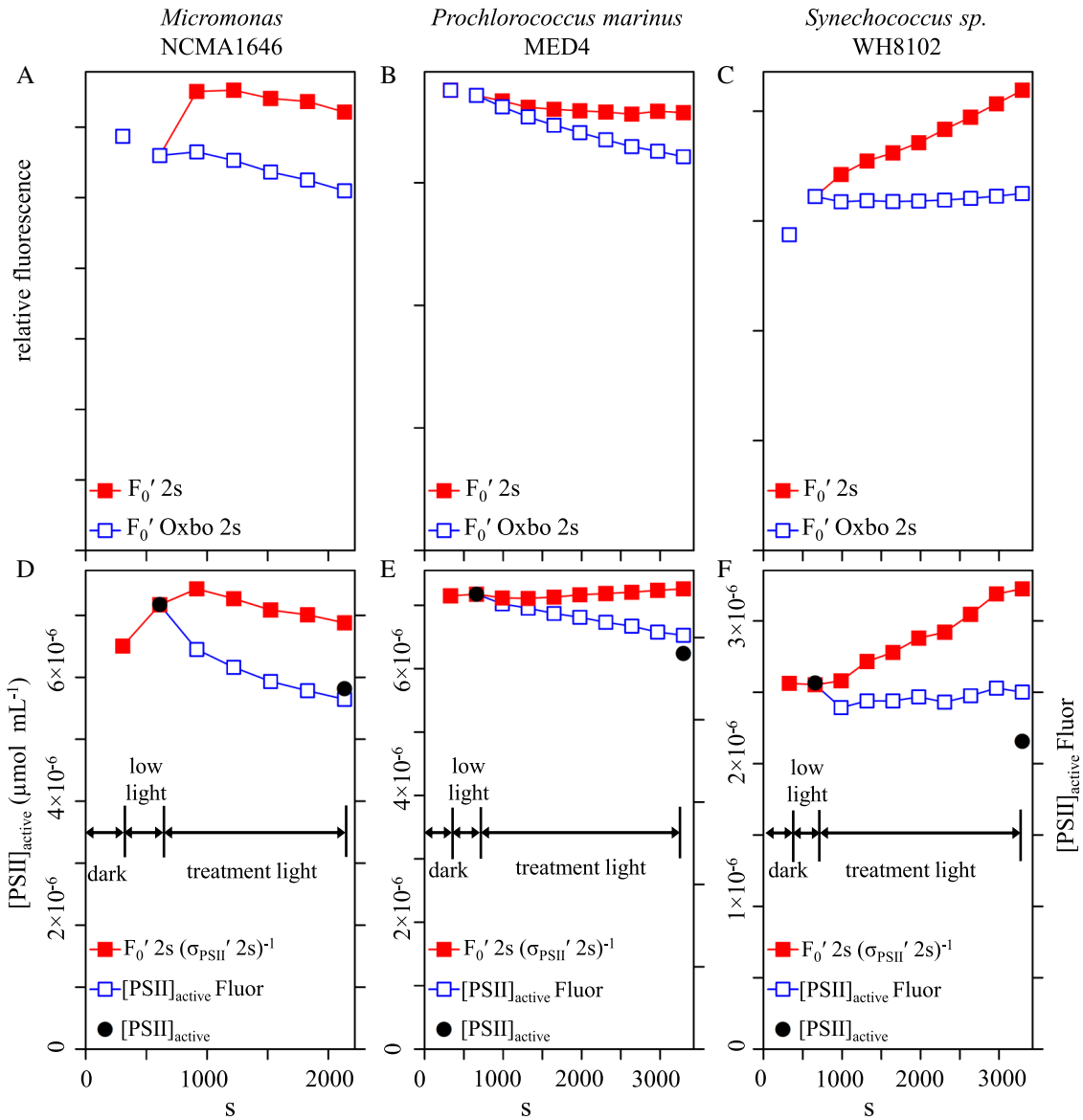

Fig. 5. Representative time courses of F_0' 2s (red squares) compared with F_0' Oxbo 2s (open blue squares) (**A**, **B**, **C**); $[PSII]_{active}$ (closed black circles) (**D**, **E**, **F**; left *y* axis); F_0' 2s/σ'_{PSII} 2s (red squares) D, E, F, right *y* axis) and relative $[PSII]_{active}$ Fluor (=F_0' Oxbo 2s/σ'_{PSII} 2s) (open blue squares) (D, E, F right *y* axis) taken from three representative light shift experiments, in the presence of lincomycin to block Photosystem II repair. Measurements were performed on *Micromonas pusilla* NCMA1646 (A, D), *Prochlorococcus marinus* MED4 (B, E), and *Synechococcus* sp. WH8102 (C, F). *Micromonas* measurements were performed on a culture grown under 185 μmol photons m^{-2} s^{-1} shifted to 400 μmol photons m^{-2} s^{-1}. *Prochlorococcus* measurements were taken from a culture grown under 30 μmol photons m^{-2} s^{-1} shifted to 260 μmol photons m^{-2} s^{-1}. *Synechococcus* measurements were taken from a culture grown under 30 μmol photons m^{-2} s^{-1} shifted to 260 μmol photons m^{-2} s^{-1}. For graphical clarity, the scale of the *y* axes of $[PSII]_{active}$ Fluor was set so that the measurement taken after low light lines up with the $[PSII]_{active}$ measure taken after low light.

relation between F_0'/σ'_{PSII} and oxygen flash yield measures of $[PSII]_{active}$.

The influence of photoinhibition on F_0'

Intriguingly photoinhibition time-course treatments caused an increase in the intercepts of our correlations (open symbols, dotted regression line; Fig. 3 ($p<0.01$), Fig. 4 ($p<0.001$)). Photoinhibition causes a rise in F_0' (Oxborough and Baker 1997; Ware et al. 2015a,b) through an increase in the fluorescence yield of photoinactivated PSII, unrelated to any increase in $[PSII]_{active}$ (Fig. 5A–C; red squares). This rise leads to a discrepancy between F_0' 2s/σ'_{PSII} 2s and $[PSII]_{active}$ determined from oxygen flash yields unrelated to any increase in $[PSII]_{active}$ (Fig. 5D–F; red squares).

(Oxborough and Baker 1997) derived an estimator of F_0' (Table 2) that excludes the cumulative influence of

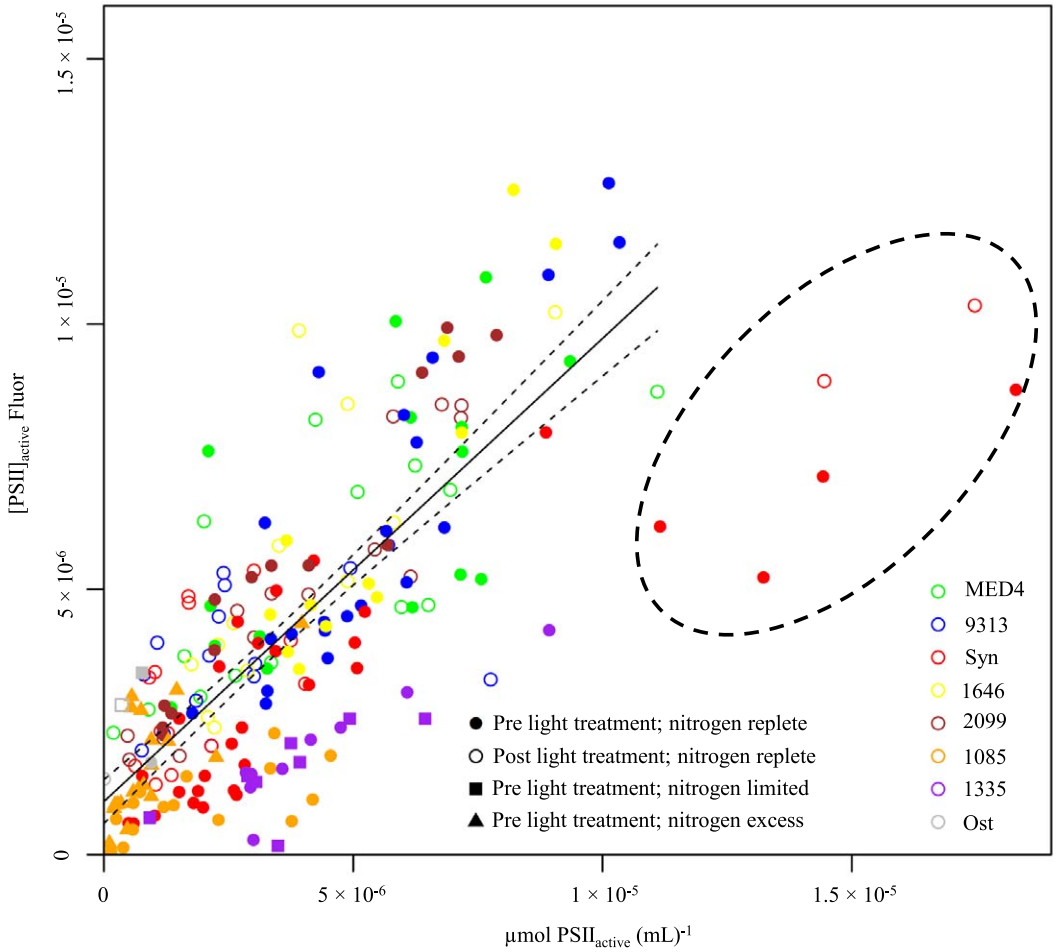

Fig. 6. The calibration of $[PSII]_{active}$ Fluor against the measured $[PSII]_{active}$ content determined via oxygen flash yield measurements. Full circles show measurements taken before the light treatment while the empty circles show measurements taken after the light treatment, both circles showing nitrogen replete conditions. Squares show nitrogen limited conditions and triangles show nitrogen excess. The data is taken from eight taxa indicated by different colored points, *Prochlorococcus marinus* MED4; *Prochlorococcus marinus* MIT9313; *Synechococcus* sp. WH8102; *Micromonas* sp. NCMA1646; *Micromonas* sp. NCMA2099; *Ostreococcus tauri* RCC745; *Thalassiosira punctigera* CCAP1085/19; and *Thalassiosira pseudonana* CCMP 1335. The solid black line shows the regression through the entire data set, with dashed lines showing 95% confidence intervals, with a slope of 0.8891 ± 0.04620 and an intercept of $1.170 \times 10^{-6} \pm 1.969 \times 10^{-7}$ and an R^2 of 0.6415. No significant effect of the light treatment ($p > 0.05$) was seen on the regression (dotted line) when fit to a linear model of $[PSII]_{active}$ Fluor against the measured $[PSII]_{active}$ with light treatment as a binary interaction term in the *R* scripting environment.

photoinactivation relative to a starting measure of F_0. Therefore, for the data measured after higher light incubations, we calculated F_0' Oxbo 2s (Fig. 5A–C) as, F_0 2s/{(F_M 2s − F_0 2s)/(F_M 2s) + (F_0 2s)/(F_M' 2s)} where the reference levels of F_0 2s and F_M 2s were measured within 2 s after initial exposure to low light (~30 μmol photons m^{-2} s^{-1}); and F_M' 2s was measured after the higher light treatment incubation. For our set of phytoplankton taxa we used F_0 2s and F_M 2s measured after exposure to initial low light because the cyanobacterial and diatom samples generally showed significant increases (Campbell et al. 1998) in F_0 2s and F_M 2s under low light compared to darkness, while the other taxa showed very little change in F_0 2s and F_M 2s from darkness to low light.

F_0' Oxbo 2s was then substituted place of F_0' 2s to counter the effect of PSII photoinhibition during our treatment time courses. For our samples taken straight from culture and measured just after exposure to growth light, F_0' Oxbo 2s is arithmetically equivalent to F_0' 2s since F_0' Oxbo 2s only accounts for photoinhibition accumulated relative to a starting control point. While this approach does not exclude variations in F_0' 2s caused by different degrees of starting photoinhibition in the cultures, our cultures were generally in exponential growth with FRR fluorescence measures of F_V/F_M expected for these taxa (Suggett et al. 2009b). We thus had little evidence of sustained photoinhibition under most growth conditions, with the exception of the diatom samples under excess N.

Time course plots of F_0' Oxbo 2s/σ'_{PSII} 2s (hereafter termed $[PSII]_{active}$ Fluor) showed an improved correlation with the oxygen flash yield measures of $[PSII]_{active}$ (Fig. 5D–F; blue squares) before

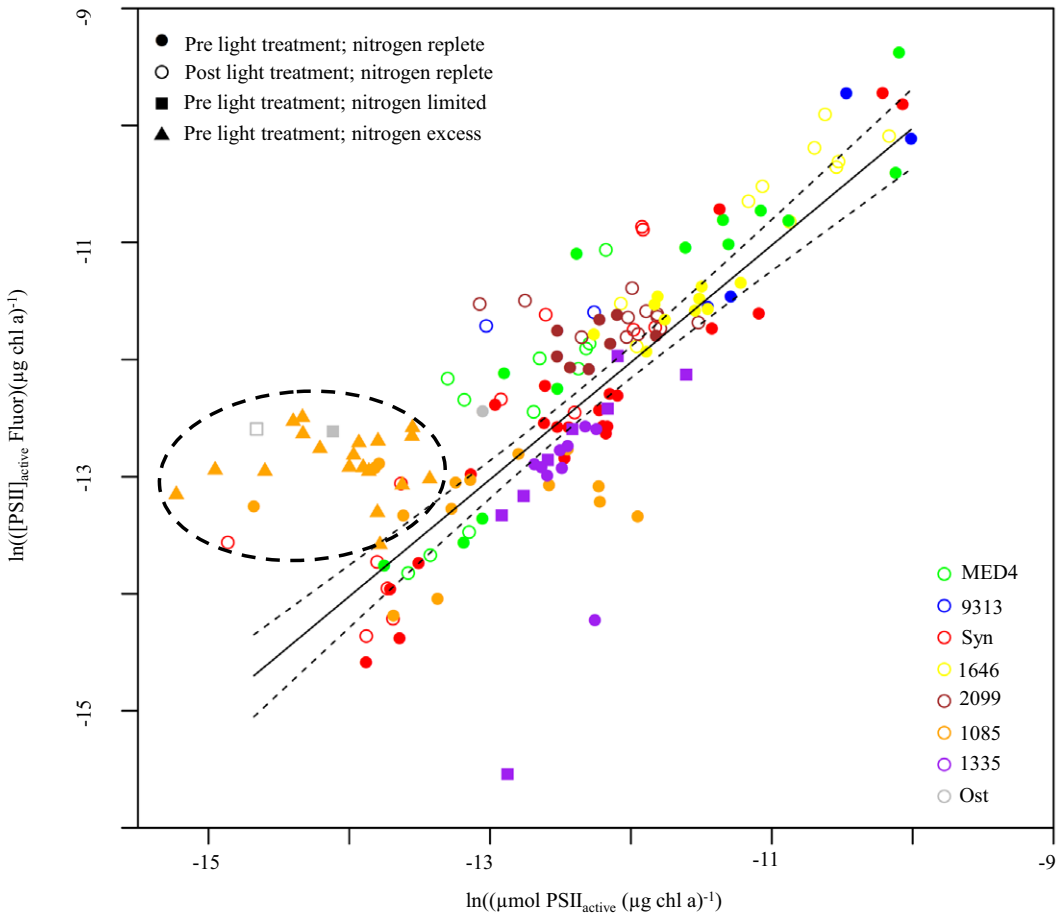

Fig. 7. The calibration of $[PSII]_{active}$ Fluor normalized to chlorophyll against the measured $[PSII]_{active}$ content determined via oxygen flash yield measurements normalized to chlorophyll. After both axes have normalized to their measured chlorophyll concentration and then the natural logarithm of the data was taken to better visualize the trend. Full symbols show measurements taken before a light treatment while the empty symbols show measurements taken after a light treatment. Circles, squares, and triangles show samples grown under nitrogen replete, limited nitrogen, and excess nitrogen, respectively. The data is taken from eight taxa indicated by different colored points, *Prochlorococcus marinus* MED4; *Prochlorococcus marinus* MIT9313; *Synechococcus* sp. WH8102; *Micromonas* sp. NCMA1646; *Micromonas* sp. NCMA2099; *Ostreococcus tauri* RCC745; *Thalassiosira punctigera* CCAP1085/19; and *Thalassiosira pseudonana* CCMP 1335. The solid black line shows the regression through the entire data set except the nitrogen excess treated data from *Thalassiosira punctigera* and the nitrogen-limited data from *Ostreococcus tauri*, with dashed lines showing 95% confidence intervals, with a slope of 1.324 ± 0.05952 and a y intercept $= 6.491 \times 10^{-8} \pm 6.895 \times 10^{-7}$ that is not significantly different from zero ($p < 0.05$) and an R^2 of 0.7845. A small significant effect of the post light treatment was seen on the intercept of the regression (dotted line) ($p > 0.05$) when fit to a linear model of $\ln([PSII]_{active}$ Fluor) against the measured $\ln([PSII]_{active}$ μg chl^{-1}) with light treatment as a binary interaction term in the *R* scripting environment.

and after photoinhibitory treatments, particularly for *Micromonas* and *Prochlorococcus*, when compared to plots of F_0' 2s/σ'_{PSII} 2s.

In *Synechococcus* photoinhibition experiments (e.g., Fig. 5C,F) $[PSII]_{active}$ Fluor exhibited improved correlation with $[PSII]_{active}$ from oxygen flash yields compared to the more simple F_0' 2s/σ'_{PSII} 2s. Nevertheless, our findings for *Synechococcus* after photoinhibition showed more variability than other taxa. We suspect cyanobacterial complexities of overlapping fluorescence emissions from PSII, Phycobiliproteins and Photosystem I, light/dark state transitions and Orange Carotenoid Protein quenching (Campbell et al. 1998; Joshua et al. 2005; Papageorgiou et al. 2007; Simis et al. 2012; Kirilovsky 2015) show complex interactions with photoinhibition that degrade the general correlation between $[PSII]_{active}$ Fluor and $[PSII]_{active}$ from oxygen flash yields. Spectrally resolved analyses of F_0' to focus on the direct PSII contribution (Simis et al. 2012) would improve the correlation; unfortunately such data is not available for our current data set which was measured with a single standard blue LED to excite fluorescence.

Calibration of $[PSII]_{active}$ Fluor using oxygen flash yield determination of $[PSII]_{active}$

$[PSII]_{active}$ Fluor plotted vs. $[PSII]_{active}$ mL^{-1} from oxygen flash yield measures (Fig. 6) showed a linear regression (solid line; $R^2 = 0.6415$; slope $= 0.8891 \pm 0.04620$, intercept $= 1.170 \times 10^{-6} \pm 1.969 \times 10^{-7}$; dotted lines show 95% confidence

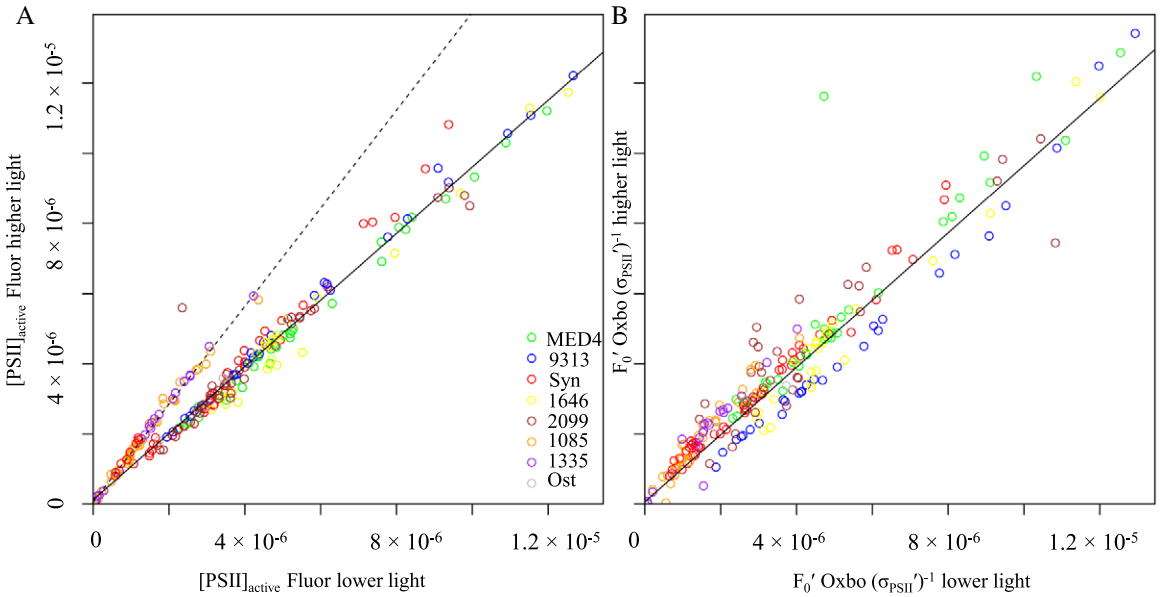

Fig. 8. Fluorescence based $[PSII]_{active}$ measured under lower and higher light. (**A**) $[PSII]_{active}$ Fluor (=(F_0' Oxbo 2s/σ'_{PSII} 2s)). The X axes show measurements taken after 5 min of lower light (30–150 μmol photons m^{-2} s^{-1}, depending on prior growth light) and thus lower Non-Photochemical Quenching. The Y axes show measurements from the same samples taken after an additional 5 min of higher treatment light (260–500 μmol photons m^{-2} s^{-1}, depending on prior growth light) and thus generally higher Non-Photochemical Quenching. The data is taken from eight taxa indicated by different colored points, *Prochlorococcus marinus* MED4; *Prochlorococcus marinus* MIT9313; *Synechococcus* sp. WH8102; *Micromonas* sp. NCMA1646; *Micromonas* sp. NCMA2099; *Ostreococcus tauri* RCC745; *Thalassiosira punctigera* CCAP1085/19; and *Thalassiosira pseudonana* CCMP 1335. The shift from lower to higher light caused a statistically significant increase in measured $[PSII]_{active}$ Fluor ($p < 0.001$) for *T. punctigera* and *T. pseudonana* (dotted line, $R^2 = 0.9936$, slope = 1.396 ± 0.016, intercept = $5.564 \times 10^{-8} \pm 2.759 \times 10^{-8}$). In contrast $[PSII]_{active}$ Fluor measured under low and higher light for the other species fell on a common regression (solid line, $R^2 = 0.9693$, slope = 0.9496 ± 0.013, *y* intercept = $1.158 \times 10^{-7} \pm 6.939 \times 10^{-8}$) with a slope slightly less than 1, indicating a slight decrease in measured $[PSII]_{active}$ Fluor under higher light compared to low light. The statistical effect was detected using a linear model for the regression with the inclusion of the two diatom species as a binary interaction term in the *R* scripting environment. (**B**) Analogous measurements performed during illumination (F_0' Oxbo/σ'_{PSII}) rather than after 2 s of dark (A). Under these conditions, there is a single pooled regression (solid line, $R^2 = 0.9108$, slope = 0.9588, *y* intercept = $6.076 \times 10^{-8} \pm 9.525 \times 10^{-8}$) with a slope slightly less than one indicating a slight decrease in measured (F_0' Oxbo/σ'_{PSII}) under higher light compared to low light. Although *T. punctigera* and *T. pseudonana* no longer showed a significant difference from the pooled regression, there is an increase in the overall scatter for the measures under illumination (lower R^2 compared to A) and the diatom points still fall on the high side of the regression.

interval on regression). The post light treatment showed no statistically significant effect on the intercept ($p > 0.05$) nor on the slope of this regression.

When we plotted $[PSII]_{active}$ Fluor normalized to μg chlorophyll *a* vs. $[PSII]_{active}$ chl^{-1} from oxygen flash yield measures (Fig. 7, the natural logarithm is taken for ease of visualizations); a strong linear trend is again seen (solid line; $R^2 = 0.7845$, slope = 1.324 ± 0.05952, *y* intercept = $6.491 \times 10^{-8} \pm 6.895 \times 10^{-7}$ was not statistically significant from zero [$p > 0.05$]; dotted lines show 95% confidence interval on regression). For the plot of $[PSII]_{active}$ Fluor normalized to chlorophyll the post light treatment retained a small, but significant effect on the intercept (open symbols; dotted regression line; $p < 0.01$). We thus found an overall correlation between $[PSII]_{active}$ Fluor and $[PSII]_{active}$ that was robust in the face of accumulated photoinactivation of PSII (Figs. 6 and 7). Our modified approach demonstrates that $[PSII]_{active}$ mL^{-1} can be retrieved form FRR fluorescence parameters with $R^2 = 0.6415$ for a single regression, applicable to control or photoinhibited samples, compared to $R^2 = 0.5627$ for control samples and a significantly different regression for photoinhibited samples, when using the previous F_0' 2s/σ'_{PSII} 2s approach (Oxborough et al. 2012; Silsbe et al. 2015).

Influence of light and non-photochemical quenching on $[PSII]_{active}$ Fluor

In Fig. 8A we plot $[PSII]_{active}$ Fluor when measured within 2 s after initial exposure to a low light, with lower yield of non-photochemical quenching (YNPQ), compared to $[PSII]_{active}$ Fluor measured within 2 s after exposure to a short period of higher treatment light, with generally more induction of YNPQ. The shift from lower to higher light caused a statistically significant increase in measured $[PSII]_{active}$ Fluor ($p < 0.001$) for the diatoms *T. punctigera* and *T. pseudonana* (dotted line, $R^2 = 0.9936$, slope = 1.396 ± 0.016, intercept = $5.564 \times 10^{-8} \pm 2.759 \times 10^{-8}$). In contrast $[PSII]_{active}$ Fluor measured under low and higher light for the other species fell on a common regression (solid line, $R^2 = 0.9693$, slope = 0.9496 ± 0.013, *y* intercept = $1.158 \times 10^{-7} \pm 6.939 \times 10^{-8}$) with a slope slightly less than 1, indicating a slight

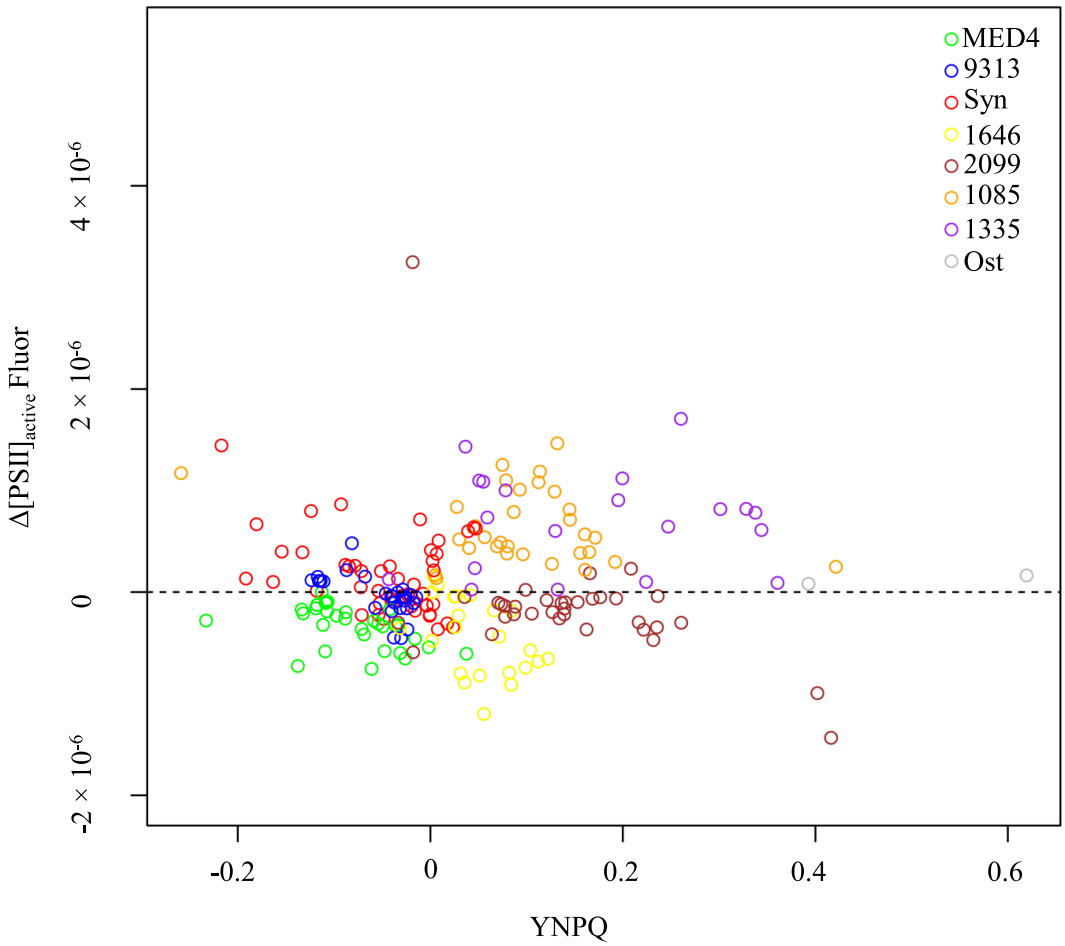

Fig. 9. Δ $[PSII]_{active}$ Fluor under high vs. low light, plotted against YNPQ. Δ $[PSII]_{active}$ Fluor is the difference between $[PSII]_{active}$ Fluor measured after 5 min of higher treatment light and $[PSII]_{active}$ Fluor measured after 5 min of low light. YNPQ = 1 − ((F'_M-F_S)/F'_M) − (F_S/$F'_{MLow\ Light}$) was calculated using low light as the baseline to show the induction of YNPQ from low to higher treatment light. The data is taken from eight taxa indicated by different coloured points, *Prochlorococcus marinus* MED4; *Prochlorococcus marinus* MIT9313; *Synechococcus* sp. WH8102; *Micromonas* sp. NCMA1646; *Micromonas* sp. NCMA2099; *Ostreococcus tauri* RCC745; *Thalassiosira punctigera* CCAP1085/19; and *Thalassiosira pseudonana* CCMP 1335. There was no correlation between Δ $[PSII]_{active}$ Fluor and YNPQ.

decrease in measured $[PSII]_{active}$ Fluor under higher light compared to low light.

In Fig. 8B we present the analogous comparison of F'_0 Oxbo/σ'_{PSII} measured directly during illumination, rather than after 2 s of dark (**8a**). Under these conditions, there is a single pooled regression (solid line, $R^2 = 0.9108$, slope = 0.9588, y intercept = $6.076 \times 10^{-8} \pm 9.525 \times 10^{-8}$) with a slope slightly less than one, indicating a slight overall decrease in F'_0 Oxbo/σ'_{PSII} measured under higher light compared to low light. Although *T. punctigera* and *T. pseudonana* no longer showed a significant difference from the pooled regression, there is an increase in the overall scatter compared to Fig. 8A and the diatom points fall on the high side of the regression. Thus measurement of $[PSII]_{active}$ Fluor immediately after illumination (as used for other figures), or measurement during illumination has only modest effects on the metric F'_0 Oxbo/σ'_{PSII}. A progression from initial limiting light to short-term exposure to saturating light also has only limited effects on the metric.

In Fig. 9 we compare the change, Δ $[PSII]_{active}$ Fluor to the YNPQ, in cultures exposed to high vs. low light. Across our panel of taxa and growth conditions there was no correlation between Δ $[PSII]_{active}$ Fluor and YNPQ, so $[PSII]_{active}$ Fluor determinations remain robust in the face of induction of variable degrees of non-photochemical quenching.

Conclusions

We confirm and build on earlier work (Oxborough et al. 2012; Silsbe et al. 2015) to generate a parameter $[PSII]_{active}$ Fluor (F'_0 Oxbo 2s/σ'_{PSII} 2s) which is predictive of $[PSII]_{active}$ whether normalized to volume or to chlorophyll across 7 diverse marine phytoplankton species; *P. marinus* MED4, *P. marinus* MIT9313, *Synechococcus* sp. WH8102, *Micromonas* sp. NCMA1646, *Micromonas* sp. NCMA2099, *T. punctigera* CCAP

1085/19, and *T. pseudonana* CCMP 1335 grown under various conditions. The prediction holds true for samples taken from exponential growth but also for samples during non-steady state progressive photoinhibition of PSII. Estimation of $[PSII]_{active}$ Fluor for marine cyanobacteria under photoinhibitory conditions showed scatter in the correlation to $[PSII]_{active}$ determined from oxygen flash yields. Consequently, future work with spectrally resolved analyses to discriminate between PSII, PSI and phycobilisome fluorescence will likely be required to generate a more robust estimator for cyanobacteria. Nevertheless, even with caveats for photoinhibited cyanobacteria, the broad regression means that our modified approach is not limited to mono-algal samples in laboratory settings but applicable for determining levels of $[PSII]_{active}$ and short-term fluctuations in $[PSII]_{active}$ across non-steady state samples, even at low cell densities or communities with multiple constituents. $[PSII]_{active}$ Fluor shows only limited change in some taxa in response to increasing background light, and shows no correlation with the level of Non-Photochemical Quenching measured concurrently in the same samples. As such $[PSII]_{active}$ Fluor is an improved platform with which to estimate $[PSII]_{active}$, and therefore determine absolute productivity using FRR fluorometry even under fluctuating conditions in lakes and oceans.

References

Babin, M., A. Morel, H. Claustre, A. Bricaud, Z. Kolber, and P. G. Falkowski. 1996. Nitrogen- and irradiance-dependent variations of the maximum quantum yield of carbon fixation in eutrophic, mesotrophic and oligotrophic marine systems. Deep-Sea Res. Part I Oceanogr. Res. Pap. **43**: 1241–1272. doi:10.1016/0967-0637(96)00058-1

Berges, J. A., D. J. Franklin, and P. J. Harrison. 2001. Evolution of an artificial seawater medium: Improvements in enriched seawater, artificial water over the last two decades. J. Phycol. **37**: 1138–1145. doi:10.1046/j.1529-8817.2001.01052.x

Brown, C., J. MacKinnon, A. Cockshutt, T. Villareal, and D. Campbell. 2008. Flux capacities and acclimation costs in *Trichodesmium* from the Gulf of Mexico. Mar. Biol. **154**: 413–422. doi: 10.1007/s00227-008-0933-z

Campbell, D., V. Hurry, A. Clarke, P. Gustafsson, and G. Oquist. 1998. Chlorophyll fluorescence analysis of cyanobacterial photosynthesis and acclimation. Microbiol. Mol. Biol. Rev. **62**: 667–683. PMID: 9729605.

Campbell, D., A. K. Clarke, P. Gustafsson, and G. Öquist. 1999. Oxygen-dependent electron flow influences photosystem II function and psbA gene expression in the cyanobacterium *Synechococcus* sp. PCC 7942. Physiol. Plant. **105**: 746–755. doi:10.1034/j.1399-3054.1999.105420.x

Campbell, D. A., and E. Tyystjärvi. 2012. Parameterization of photosystem II photoinactivation and repair. Biochim. Biophys. Acta **1817**: 258–265. doi:10.1016/j.bbabio.2011.04.010

Campbell, D. A., Z. Hossain, A. M. Cockshutt, O. Zhaxybayeva, H. Wu, and G. Li. 2013. Photosystem II protein clearance and FtsH function in the diatom Thalassiosira pseudonana. Photosynth. Res. **115**: 43–54. doi: 10.1007/s11120-013-9809-2

Chow, W. S., A. B. Hope, and J. M. Anderson. 1989. Oxygen per flash from leaf disks quantifies photosystem II. Biochim. Biophys. Acta BBA Bioenerg. **973**: 105–108. doi: 10.1016/S0005-2728(89)80408-6

Drath, M., N. Kloft, A. Batschauer, K. Marin, J. Novak, and K. Forchhammer. 2008. Ammonia triggers photodamage of photosystem II in the cyanobacterium Synechocystis sp. strain PCC 6803. Plant Physiol. **147**: 206–215. doi: 10.1104/pp.108.117218

Falkowski, P., T. Fenchel, and E. Delong. 2008. The microbial engines that drive earth's biogeochemical cycles. Science **320**: 1034–1039. doi:10.1126/science.1153213

Guillard, R. R. L., and J. H. Ryther. 1962. Studies of Marine Planktonic Diatoms: I. Cyclotella Nana Hustedt, and Detonula Confervacea (cleve) Gran. Can. J. Microbiol **8**: 229–239. doi:10.1139/m62-029

Guillard, R. R. L., and P. E. Hargraves. 1993. *Stichochrysis immobilis* is a diatom, not a chrysophyte. Phycologia **32**: 234–236. doi:10.2216/i0031-8884-32-3-234.1

Hakkila, K., T. Antal, A. U. Rehman, J. Kurkela, H. Wada, I. Vass, E. Tyystjärvi, and T. Tyystjärvi. 2014. Oxidative stress and photoinhibition can be separated in the cyanobacterium Synechocystis sp. PCC 6803. Biochim. Biophys. Acta BBA Bioenerg. **1837**: 217–225. doi:10.1016/j.bbabio.2013.11.011

Halsey, K. H., A. J. Milligan, and M. J. Behrenfeld. 2011. Linking time-dependent carbon-fixation efficiencies in dunaliella tertiolecta (chlorophyceae) to underlying metabolic pathways1. J. Phycol. **47**: 66–76. doi:10.1111/j.1529-8817.2010.00945.x

Harrison, P. J., R. E. Waters, and F. J. R. Taylor. 1980. A broad spectrum artificial sea water medium for coastal and open ocean phytoplankton1. J. Phycol. **16**: 28–35. doi:10.1111/j.0022-3646.1980.00028.x

Huot, Y., and M. Babin. 2010. Overview of fluorescence protocols: Theory, basic concepts, and practice, p. 31–74. *In* D. J. Suggett, O. Prášil, and M. A. Borowitzka [eds.], Chlorophyll a fluorescence in aquatic sciences: Methods and applications. Springer.

Jeffrey, S., and G. Humphrey. 1975. New spectrophotometric equations for determining chlorophylls a1, b1, c1 and c2 in higher plants, algae and natural phytoplankton. Biochem. Physiol. Pflanz. **167**: 191–194. doi: 10.1111/j.0022-3646.1980.00028.x

Joshua, S., S. Bailey, N. H. Mann, and C. W. Mullineaux. 2005. Involvement of phycobilisome diffusion in energy quenching in cyanobacteria. Plant Physiol. **138**: 1577–1585. doi:10.1104/pp.105.061168

Keller, M. D., R. C. Selvin, W. Claus, and R. R. L. Guillard. 1987. Media for the culture of oceanic ultraphytoplankton1,2. J. Phycol. **23**: 633–638. doi:10.1111/j.1529-8817.1987.tb04217.x

Key, T., A. Mccarthy, D. Campbell, C. Six, S. Roy, and Z. Finkel. 2010. Cell size trade-offs govern light exploitation strategies in marine phytoplankton. Environ. Microbiol. **12**: 95–104. doi:10.1111/j.1462-2920.2009.02046.x

Kirilovsky, D. 2015. Modulating energy arriving at photochemical reaction centers: Orange carotenoid protein-related photoprotection and state transitions. Photosynth. Res. **126**: 3–17. doi:10.1007/s11120-014-0031-7

Kolber, Z. S., O. Prášil, and P. G. Falkowski. 1998. Measurements of variable chlorophyll fluorescence using fast repetition rate techniques: Defining methodology and experimental protocols. Biochim. Biophys. Acta BBA Bioenerg. **1367**: 88–106. doi:10.1016/S0005-2728(98)00135-2

van Kooten, O., and J. F. H. Snel. 1990. The use of chlorophyll fluorescence nomenclature in plant stress physiology. Photosynth. Res. **25**: 147–150. doi:10.1007/BF00033156

Laney, S. R. 2003. Assessing the error in photosynthetic properties determined with fast repetition rate fluorometry. Limnol. Oceanogr. **48**: 2234–2242. doi:10.4319/lo.2003.48.6.2234

Laney, S. R., and R. M. Letelier. 2008. Artifacts in measurements of chlorophyll fluorescence transients, with specific application to fast repetition rate fluorometry. Limnol. Oceanogr. Methods **6**: 40–50. doi:10.4319/lom.2008.6.40

Lavaud, J. 2007. Fast regulation of photosynthesis in diatoms: Mechanisms, evolution and ecophysiology. Functional Plant Science and Biotechonology **1**: 267–287.

Lawrenz, E., and others. 2013. Predicting the electron requirement for carbon fixation in seas and oceans. PLoS One **8**: e58137. doi:10.1371/journal.pone.0058137

Macey, A. I., T. Ryan-Keogh, S. Richier, C. M. Moore, and T. S. Bibby. 2014. Photosynthetic protein stoichiometry and photophysiology in the high latitude North Atlantic. Limnol. Oceanogr. **59**: 1853–1864. doi:10.4319/lo.2014.59. 6.1853

Moore, C. M., D. J. Suggett, A. E. Hickman, Y.-N. Kim, J. F. Tweddle, J. Sharples, R. J. Geider, and P. M. Holligan. 2006. Phytoplankton photoacclimation and photoadaptation in response to environmental gradients in a shelf sea. Limnol. Oceanogr. **51**: 936–949. doi:10.4319/lo.2006.51.2.0936

Moore, C. M., and others. 2013. Processes and patterns of oceanic nutrient limitation. Nat. Geosci. **6**: 701–710. doi:10.1038/ngeo1765

Oliver, R. L., J. Whittington, Z. Lorenz, and I. T. Webster. 2003. The influence of vertical mixing on the photoinhibition of variable chlorophyll a fluorescence and its inclusion in a model of phytoplankton photosynthesis. J. Plankton Res. **25**: 1107–1129. doi:10.1093/plankt/25.9.1107

Oxborough, K., and N. R. Baker. 1997. Resolving chlorophyll a fluorescence images of photosynthetic efficiency into photochemical and non-photochemical components – calculation of qP and Fv′/Fm′; without measuring Fo′. Photosynth. Res. **54**: 135–142. doi:10.1023/A:1005936823310

Oxborough, K., C. M. Moore, D. J. Suggett, T. Lawson, H. G. Chan, and R. J. Geider. 2012. Direct estimation of functional PSII reaction center concentration and PSII electron flux on a volume basis: A new approach to the analysis of Fast Repetition Rate fluorometry (FRRf) data. Limnol. Oceanogr. Methods **10**: 142–154. doi:10.4319/lom.2012.10.142

Papageorgiou, G. C., M. Tsimilli-Michael, and K. Stamatakis. 2007. The fast and slow kinetics of chlorophyll a fluorescence induction in plants, algae and cyanobacteria: A viewpoint. Photosynth. Res. **94**: 275–290. doi:10.1007/s11120-007-9193-x

Ritchie, R. J. 2006. Consistent sets of spectrophotometric chlorophyll equations for acetone, methanol and ethanol solvents. Photosynth. Res. **89**: 27–41. doi:10.1007/s11120-006-9065-9

Roberty, S., B. Bailleul, N. Berne, F. Franck, and P. Cardol. 2014. PSI Mehler reaction is the main alternative photosynthetic electron pathway in *Symbiodinium* sp., symbiotic dinoflagellates of cnidarians. New Phytol. **204**: 81–91. doi:10.1111/nph.12903

Shoaf, W. T., and B. W. Lium. 1976. Improved extraction of chlorophyll a and b from algae using dimethyl sulfoxide. Limnol. Oceanogr. **21**: 926–928. doi:10.4319/lo.1976.21.6.0926

Silsbe, G. M., and others. 2015. Toward autonomous measurements of photosynthetic electron transport rates: An evaluation of active fluorescence-based measurements of photochemistry. Limnol. Oceanogr. Methods **13**: 138–155. doi:10.1002/lom3.10014

Simis, S. G. H., Y. Huot, M. Babin, J. Seppälä, and L. Metsamaa. 2012. Optimization of variable fluorescence measurements of phytoplankton communities with cyanobacteria. Photosynth. Res. **112**: 13–30. doi:10.1007/s11120-012-9729-6

Smith, B. M., P. J. Morrissey, J. E. Guenther, J. A. Nemson, M. A. Harrison, J. F. Allen, and A. Melis. 1990. Response of the photosynthetic apparatus in *Dunaliella salina* (green algae) to irradiance stress. Plant Physiol. **93**: 1433–1440. doi:10.1104/pp.93.4.1433

Suggett, D., H. MacIntyre, and R. Geider. 2004. Evaluation of biophysical and optical determinations of light absorption by photosystem II in phytoplankton. Limnol. Oceanogr. Methods **2**: 316–332. doi:10.4319/lom.2004.2.316

Suggett, D. J., S. C. Maberly, and R. J. Geider. 2006. Gross photosynthesis and lake community metabolism during the spring phytoplankton bloom. Limnol. Oceanogr. **51**: 2064–2076. doi:10.4319/lo.2006.51.5.2064

Suggett, D., H. MacIntyre, T. Kana, and R. Geider. 2009a. Comparing electron transport with gas exchange: Parameterising exchange rates between alternative photosynthetic currencies for eukaryotic phytoplankton. Aquat. Microb. Ecol. **56**: 147–162. doi:10.3354/ame01303

Suggett, D., C. Moore, A. Hickman, and R. Geider. 2009b. Interpretation of fast repetition rate (FRR) fluorescence: Signatures of phytoplankton community structure versus physiological state. Mar. Ecol. Prog. Ser. **376**: 1–19. doi:10.3354/meps07830

Suggett, D. J., C. M. Moore, and R. J. Geider. 2010. Estimating aquatic productivity from active fluorescence measurements, p. 103–127. *In* D. J. Suggett, O. Prášil, and M. A. Borowitzka [eds.], Chlorophyll a fluorescence in aquatic sciences: Methods and applications. Springer.

Tyystjärvi, T., I. Tuominen, M. Herranen, E.-M. Aro, and E. Tyystjärvi. 2002. Action spectrum of *psbA* gene transcription is similar to that of photoinhibition in *Synechocystis* sp. PCC 6803. FEBS Lett. **516**: 167–171. doi:10.1016/S0014-5793(02)02537-1

Ware, M. A., E. Belgio, and A. V. Ruban. 2015a. Photoprotective capacity of non-photochemical quenching in plants acclimated to different light intensities. Photosynth. Res. **126**: 261–274. doi:10.1007/s11120-015-0102-4

Ware, M. A., E. Belgio, and A. V. Ruban. 2015b. Comparison of the protective effectiveness of NPQ in Arabidopsis plants deficient in PsbS protein and zeaxanthin. J. Exp. Bot. **66**: 1259–1270. doi:10.1093/jxb/eru477

Waring, J., M. Klenell, U. Bechtold, G. J. C. Underwood, and N. R. Baker. 2010. Light-induced responses of oxygen photoreduction, reactive oxygen species production and scavenging in two diatom species. J. Phycol. **46**: 1206–1217. doi:10.1111/j.1529-8817.2010.00919.x

Welschmeyer, N. A. 1994. Fluorometric analysis of chlorophyll a in the presence of chlorophyll b and pheopigments. Limnol. Oceanogr. **39**: 1985–1992. doi:10.4319/lo.1994.39.8.1985

Wu, H., A. M. Cockshutt, A. McCarthy, and D. A. Campbell. 2011. Distinctive photosystem II photoinactivation and protein dynamics in marine diatoms. Plant Physiol. **156**: 2184–2195. doi:10.1104/pp.111.178772

Wu, H., S. Roy, M. Alami, B. R. Green, and D. A. Campbell. 2012. Photosystem II photoinactivation, repair, and protection in marine centric diatoms. Plant Physiol. **160**: 464–476. doi:10.1104/pp.112.203067

Acknowledgments

Dr. K. Oxborough, Chelsea Instruments and D. Ware, Imperial College London were generous in discussions helping to advance our thinking on parameterizations of $[PSII]_{active}$. The authors thank Dr. E. Austen, Mount Allison University/University of Ottawa and Dr. M. Thaler, Université Laval, for advice on R coding. T. Burris and P. Shaver of Mount Allison University did pilot experiments for this project as part of their honours theses work. This work was funded by the Canada Research Chair program (DC), using equipment funded by the Canada Foundation for Innovation and the New Brunswick Foundation for Innovation (DC). C.D. Murphy and J. Grant-Burt were supported by summer fellowships from Mount Allison University. NSERC Engage funding supported A. Barnett to write the PSIWORX-R scripts for extracting chlorophyll fluorescence induction and relaxation parameters from data generated by PSI Fluorometers, with sponsorship from QuBit Systems, Kingston, Ontario. The contribution of DJS was supported through an Australian Research Council (ARC) Future Fellowship (FT130100202). The contribution of JL was supported by the Marine Microbiology Initiative of the Gordon & Betty Moore Foundation.

Conflict of Interest

None declared.

Submitted 19 July 2016
Revised 29 August 2016
Accepted 02 September 2016

Associate editor: Tammi Richardson